RESEARCH ARTICLE

Development and characterization of a photocurable alginate bioink for three-dimensional bioprinting

H. H. Mishbak[1,2], Glen Cooper[2], P. J. Bartolo[2]*

[1]Department of Biomedical Engineering, School of Engineering, University of Thi-Qar. Thi-Qar, Iraq
[2]Manufacturing Group, School of Mechanical, Aerospace and Civil Engineering, The University of Manchester, Manchester, UK

Abstract: Alginate is a biocompatible material suitable for biomedical applications, which can be processed under mild conditions on irradiation. This paper investigates the preparation and the rheological behavior of different pre-polymerized and polymerized alginate methacrylate systems for three-dimensional photopolymerization bioprinting. The effect of the functionalization time on the mechanical, morphological, swelling, and degradation characteristics of cross-linked alginate hydrogel is also discussed. Alginate was chemically-modified with methacrylate groups and different reaction times considered. Photocurable alginate systems were prepared by dissolving functionalized alginate with 0.5- 1.5% w/v photoinitiator solutions and cross-linked by ultraviolet light (8 mW/cm^2 for 8 minutes).

Keywords: 3D bioprinting; Alginate hydrogel; Functionalization; Photopolymerization; Rheology

*Correspondence to: P. J. Bartolo, School of Mechanical, Aerospace and Civil Engineering, Manchester Biomanufacturing Centre, Manchester Institute of Biotechnology, University of Manchester, Manchester, UK; paulojorge.dasilvabartolo@manchester.ac.uk

Received: March 4, 2019; **Accepted:** March 25, 2019; **Published Online:** July 1, 2019

Citation: Mishbak HH, Cooper G, Bartolo PJ, 2019, Development and characterization of a photocurable alginate bioink for three dimensional bioprinting. Int J Bioprint, 5(2): 189. http://dx.doi.org/10.18063/ijb.v5i2.189

1. Introduction

Three different approaches are being explored for tissue engineering applications[1,2]. The first approach, cell therapy, is based on harvesting cells, sorting, expanding, and implanted them. This is a simple process but presents limited outcomes as it is difficult to keep the cells in the desired region for clinically relevant periods of time[3]. The second approach, scaffold-based approach, is based on the use of three-dimensional support structures that provide the necessary environment for cell attachment, differentiation, and proliferation[4]. In this approach, scaffolds can be directly implanted after fabrication or seeded with cells and pre-cultured in a bioreactor before implantation[5]. Finally, the third approach (bioprinting) uses bioinks (hydrogels and cells) to create cell-laden constructs. This is a highly relevant approach allowing *in situ* printing[6,7]. Technologies such as inkjet bioprinting, extrusion-based, and photopolymerization-based process are being explored. Among them, photopolymerization is a very versatile method allowing a rapid crosslinking under biocompatible reaction conditions without the use of solvents[1,6]. In addition, photocurable hydrogels are particularly relevant for biomedical applications due to the advantage of being able to encapsulate cells and the mild processing conditions that allow their *in situ* crosslinking within a patient during a surgical procedure.

Suitable hydrogels for bioprinting must be biocompatible, biodegradable, present appropriate mechanical properties, which depend on the type of tissue, good printability,[8] and shear thinning properties to facilitate the printing process[9]. In the case of photopolymerization bioprinting systems, the amount and type of photoinitiator are also critical as determines the crosslinking density, cytotoxicity, mechanical properties, and biocompatibility[10]. The increase of crosslinking density is usually associated with an increase of printability and mechanical properties and a decrease of biocompatibility due to the reduction of free space to accommodate cell proliferation[11].

Alginate is a suitable material for bioprinting[12]. It is a natural water-soluble linear polysaccharide derived from alginic acid, extracted from several species of brown algae, such as *Laminaria hyperborea*, *Ascophyllum nodosum,* and *Macrocystis pyrifera*[13-15]. Its structure contains 1,4-linked β-D-mannuronic (M) and α-L-guluronic (G) acid residues (Figure 1), arranged in a non-regular and block-wise fashion along the chain[16-18]. Alginate shows good biocompatibility, low cytotoxicity, and high-water content (high swelling ratio), mimicking the structure of the natural extracellular matrix[19-23]. These properties make alginate a suitable material for wound dressings, drug delivery systems, and soft tissue engineering applications[24].

This paper investigates the preparation of alginate-based systems for ultraviolet (UV) bioprinting applications. The material is characterized both before and after the curing process, and the effect of functionalization time on the rheological, mechanical, morphological, swelling, and degradation properties was investigated. The effect of photoinitiator concentration in terms of rheological and mechanical properties is also assessed and discussed. The biological characteristics are not reported in this manuscript, but preliminary results with human chondrocytes show that the materials considered here do not present any cytotoxicity and allow cell attachment and proliferation[26].

2. Materials and Methods

2.1 Synthesis of Methacrylate Alginate

Photocurable alginates were prepared through a functionalization mechanism with methacrylate anhydride (MA)[27]. Briefly, sodium alginate powder 1%, 2%, and 3% (w/v) (Sigma-Aldrich, UK) was dissolved in Dulbecco's phosphate-buffered saline (Sigma-Aldrich, UK) and then mixed with MA (Sigma-Aldrich, UK) at 15 mL MA/g of alginate under vigorous stirring. The pH of the solution was kept around 7.4–8.0 during the reaction time by adding 5M of NaOH. Maintaining a higher pH during the reaction is crucial since higher pH enhances the reaction among the amine and hydroxyl groups, which lead to a higher degree of modification[28]. Two different reaction times (8 and 24 h) were used to assess the effect of the reaction time on the degree of functionalization.

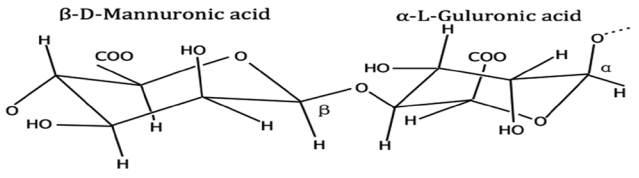

Figure 1. Alginate showing a linkage between the mannuronic and guluronic acid[25].

After the chemical modification reaction, the polymeric solution was precipitated and totally mixed in 100 mL of ethanol (100% ethanol) and dried in an oven overnight at 50°C. The precipitate polymer was dissolved in distilled water (diH_2O), loaded in the dialysis tubes membranes (SnakeSkin Dialysis Tubing from Thermo Fisher Scientific, UK), sealing both sides and dialyzed the solution against NaCl for 7 days with periodic water changes every day. The solution was freeze at −80°C and the polymer recovered by lyophilization.

2.2 Characterization of Pre-polymerized Methacrylate Alginate

2.2.1 Nuclear magnetic resonance (NMR)

The chemical structure of functionalized alginate was assessed through ^{1}HNMR spectroscopy, using the B400 Bruker Avance III 400 MHz (Billerica, Massachusetts, USA). Polymeric materials were dissolved in deuterium oxide (Sigma-Aldrich, UK), transferred to NMR tubes and the spectra acquired with 128 scans.

2.2.2 Rheological characterization

The rheological tests were performed to characterize the viscoelastic behavior of both pre-polymerized and polymerized alginate. The rheological assessment of pre-polymerized alginate systems was carried out using the DHR2 TA Instrument (USA). Samples were placed between two parallel plates and two different tests (rotational and oscillation) were considered. Rotational tests were performed to evaluate the viscosity and material strength. In these tests it is assumed that the material flows by applying stress, being the response measured alongside time (temperature was not considered in this work). Controlled stress was applied, and the resulting movement measured. Oscillation tests were considered to evaluate the viscoelastic behavior of the material and dynamic moduli. The viscoelastic behavior was characterized by measuring the energy stored (storage modulus, G′) in the material during shearing and the energy subsequently lost (loss modulus, G″). Shear strain was controlled by varying the oscillation amplitude.

To assess the rheological changes during the photopolymerization process, the rheological tests were carried out using the Bohlin Gemini system (Malvern Instruments) equipped with the OmniCure® S1000 light source irradiating in the range of 254–450 nm wavelength, and oscillation tests were considered. The light intensity was 10 mW/cm^2.

The rheological behavior of the materials is described by the following equation:

$$\tau = \eta \dot{\gamma}^n \quad (1)$$

Where τ is the $\dot{\gamma}$ shear stress (Pa), is the shear rate (s^{-1}), η the consistency index or equivalent viscosity (Pa. s), and n is the power law index (dimensionless) that varies as follows:

n<1: Shear-thinning system;
n=1: Newtonian system;
n>1: Shear-thickening system.

2.3 Hydrogel Formation

Photocrosslinked alginate methacrylate hydrogels were prepared by dissolving 2% w/v alginate methacrylate with different photoinitiator concentration solutions (0.5-1.5% w/v) of VA-086 photoinitiator solutions (2,2'-Azobis[2-methyl-N-(2-hydroxyethyl) propionamide azo initiator (Wako Pure Chemical Industries, USA). Cross-linked disks were produced by pipetting the alginate solution in an acrylic mold with 8 mm diameter and 4 mm height. Photopolymerization was conducted using a 365 nm UV light (Model Dymax 2000-EC, Dymax Europe GmbH, Wiesbaden, Germany) irradiating at 8 mW/cm^2 during 8 min.

The photopolymerization process of alginate methacrylate is a radicular polymerization process started by the absorption of UV light by the photoinitiators followed by the generation of free radicals and a cross-linking chain reaction[29]. The mechanism is briefly presented in Figure 2.

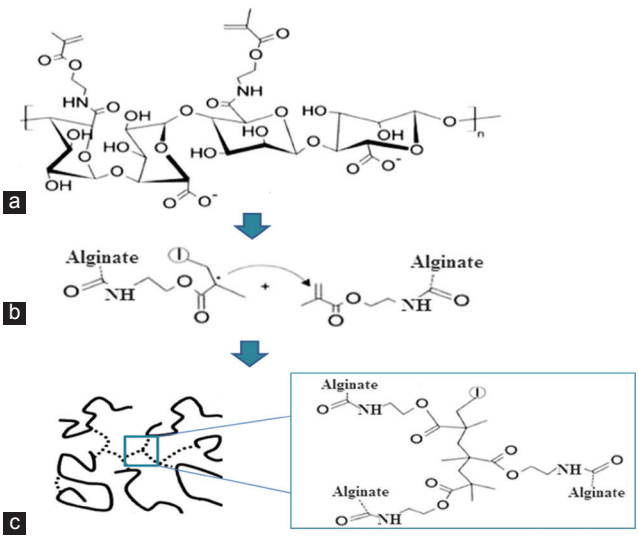

Figure 2. Schematic representation of the photopolymerization process of alginate methacrylate. (a) After exposing the polymer solution to ultraviolet radiation, the photoinitiators generated free radicals that react with the vinyl methylene starting the crosslinking reaction; (b) the reaction propagates with macroradicals reacting with unreacted carbon-carbon double bonds. (c) At the end through a bimolecular termination mechanism, a three-dimensional network of the cross-linked hydrogel is formed[30].

2.4 Characterization of Photocrosslinked Hydrogels

2.4.1 Morphological characterization

The morphology of the internal structure of the hydrogels was investigated through scanning electron microscopy (SEM), using the Hitachi S3000N VPSEM system. Alginate samples were produced using cylindrical molds (8 mm diameter and 4 mm high). After hydrogel formation, samples were extensively washed in diH_2O, frozen at −80°C and lyophilized. Samples were fixed on stubs using double-sided adhesive tape and sputter coated with platinum sputter-coating.

2.4.2 Mechanical characterization

Compression tests were performed at a constant strain rate using the Instron 3344 machine equipped with a 10-N load cell (Instron, Buckinghamshire, UK). Cross-linked alginate hydrogel disks were prepared as described in section (2.2) and maintained in diH_2O at 37ºC following the protocol described by Jeon *et al*.[27]. After 24 h of incubation, swollen alginate methacrylate hydrogel disks were measured using calipers to determine both the diameter and thickness and unconfined compression tests were performed on the hydrogel disks at room temperature, 0.5 mm/min of speed at a rate of 20% strain. Compressive modulus was determined from the slope of stress versus strain plots and limited to the first 10% of strain as recommended for cartilage applications[31].

2.4.3. Swelling and degradation characterization

Alginate methacrylate hydrogel disks were frozen at −80°C, then, lyophilized and the dry weights (Wi) were measured. Afterward, the dried hydrogel samples were immersed in diH_2O and the same number of samples were also immersed in Dulbecco's Modified Eagle's Medium (DMEM) – high glucose (Sigma-UK) diluted with 10% fetal bovine serum (Thermofisher, UK) at pH 7 and incubated at 37°C to reach an equilibrium swelling state. The diH_2O and DMEM were replaced every 1–2 days. Over the course of 3 weeks, samples were removed from the DMEM/diH_2O and the swollen hydrogel sample weights (Ws) measured. The swelling ratio (water content Q) was calculated according to the following equation:

$$Q = \frac{Ws}{Wi} \quad (2)$$

Where Wi is the dry weight and Ws is the weight of the swollen hydrogel sample. After this, the swollen hydrogels were lyophilized and weighed again. The percentage of mass loss was calculated as follows:

$$(W_i - W_d)/W_i \times 100 \quad (3)$$

Where W_d is the weight after lyophilization (n = 3 for each time point).

3. Results and Discussion

3.1 Alginate Functionalization

The alginate modification with MA was performed under standard conditions, allowing the introduction of photo-reactive methacrylate groups into the polymer backbone, as confirmed by ^{1}HNMR analysis (Figures 3-5). Results indicate the presence of new characteristic peaks of methacrylate (MA) at 5.63 ppm and 6.09 ppm attributed to the methylene group in the vinyl bond, and a peak at 1.82 ppm assigned to the methyl group, which are not present in the non-modified polymer, showing that the polymers were successfully functionalized.

Two different functionalization reaction times (8 and 24 h) were also considered and the degree of modification determined by dividing the relative integrations of methylene to carbohydrate protons[32,33]. Results, presented in Table 1, show that the degree of modification increases by increasing the reaction time, reaching a maximum value of 33% at 24 h.

3.2 Rheological Behavior of Pre-polymerized Alginate Methacrylate Systems

Figures 6-9 showed the stress versus shear rate behavior of solutions containing 1, 2, and 3% (w/v) of alginate methacrylate reacted for 8 and 24 h. Key rheological parameters are presented in Tables 2 and 3. A non-linear behavior is observed for all samples. Samples containing 2% w/v obtained after 24 h of reaction show a clear Bingham behavior[34]. Results also show a decrease of the equivalent viscosity by increasing the alginate concentration for samples obtained after 24 h of reaction, while no trend was observed for samples obtained after 8 h of reaction. The flow behavior is also closer to a Newtonian fluid for samples containing high concentrations of alginate. Based on these results, the system containing 2% w/v of alginate

Table 1. Effect of reaction time on the modification degree of alginate methacrylate

Composition (% w/v)	Reaction time (hours)	Degree of modification (%)
2%	8	21
2%	24	33

Table 2. Rheological constants for solutions containing 15 mL of methacrylate and different alginate concentrations, 24 h

Composition (%w/v)	Equivalent viscosity (Pa. s)	Power law constant
1	4.36	0.23
2	0.54	0.68
3	0.16	0.72

Table 3. Rheological constants for solutions containing 15 mL of methacrylate and different alginate concentrations, 8 h

Composition (%w/v)	Equivalent viscosity (Pa. s)	Power law constant
1	0.09	0.81
2	0.48	0.48
3	0.08	0.74

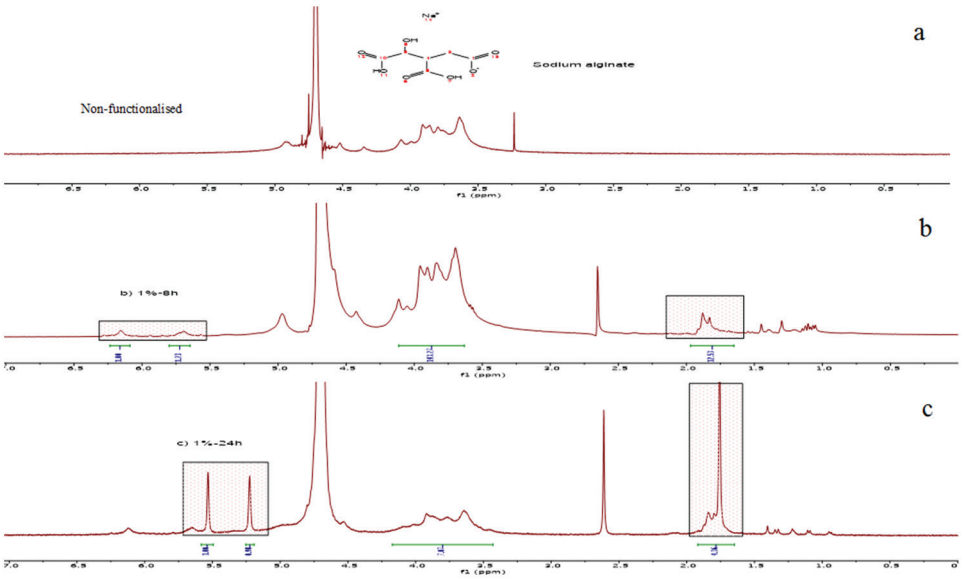

Figure 3. (a) Non-functionalized alginate (1% w/v), (b) functionalized alginate (1% w/v) after 8 h of reaction, (c) functionalized alginate (1% w/v) after 24 h of reaction. The functionalization is confirmed by the presence of new peaks in the spectra at 5.63 ppm and 6.09 ppm attributed to the methylene group and a peak at 1.82 ppm that corresponds to the methyl group.

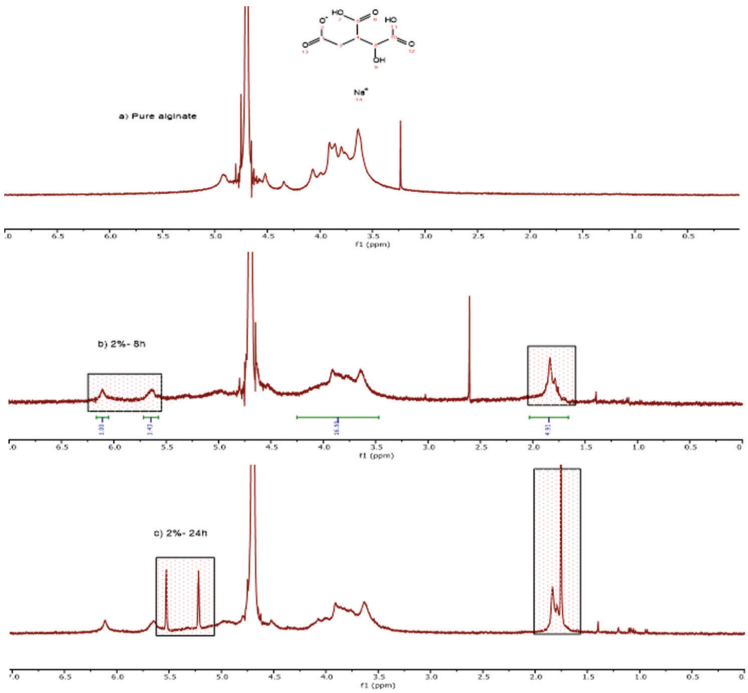

Figure 4. (a) Non-functionalized alginate (2% w/v), (b) functionalized alginate (2% w/v) after 8 h of reaction, (c) functionalized alginate (2% w/v) after 24 h of reaction. The functionalization is confirmed by the presence of new peaks in the spectra at 5.63 ppm and 6.09 ppm attributed to the methylene group and a peak at 1.82 ppm that corresponds to the methyl group.

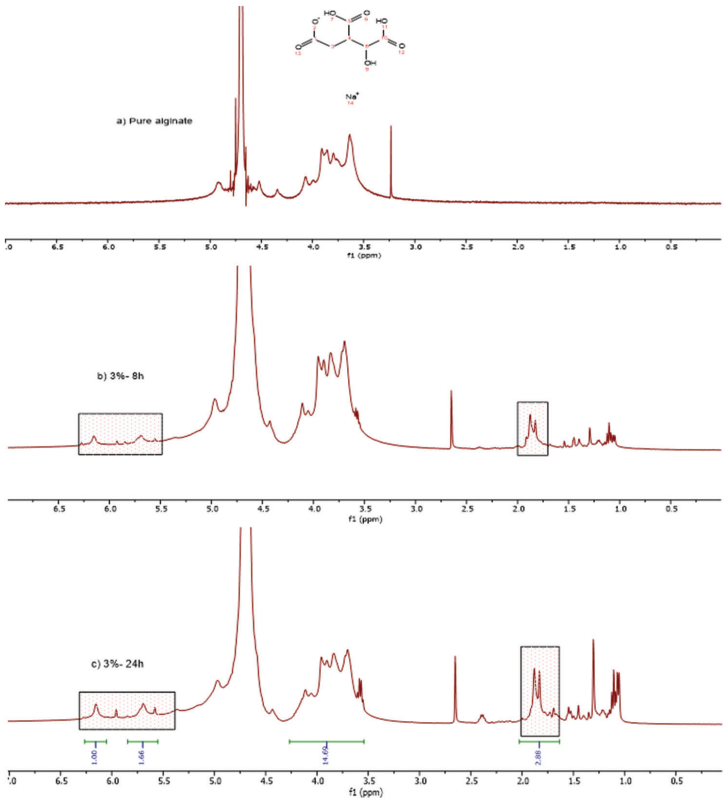

Figure 5. (a) Non-functionalized alginate (3% w/v), (b) functionalized alginate (2% w/v) after 8 h of reaction, (c) functionalized alginate (2% w/v) after 24 h of reaction. The functionalization is confirmed by the presence of new peaks in the spectra at 5.63 ppm and 6.09 ppm attributed to the methylene group and a peak at 1.82 ppm that corresponds to the methyl group.

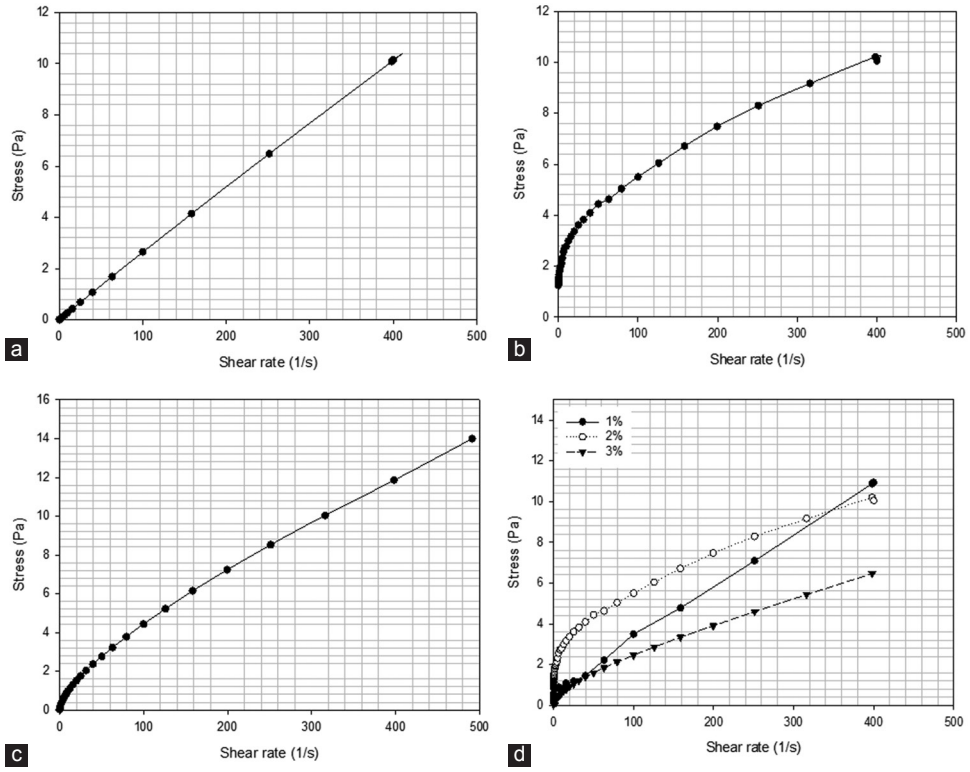

Figure 6. Stress versus shear rate profiles for alginate methacrylate solutions containing different alginate methacrylate concentrations, reacted for 8 h. (a) 1% w/v of alginate, (b) 2% w/v of alginate, (c) 3% w/v of alginate, (d) comparison of all compositions.

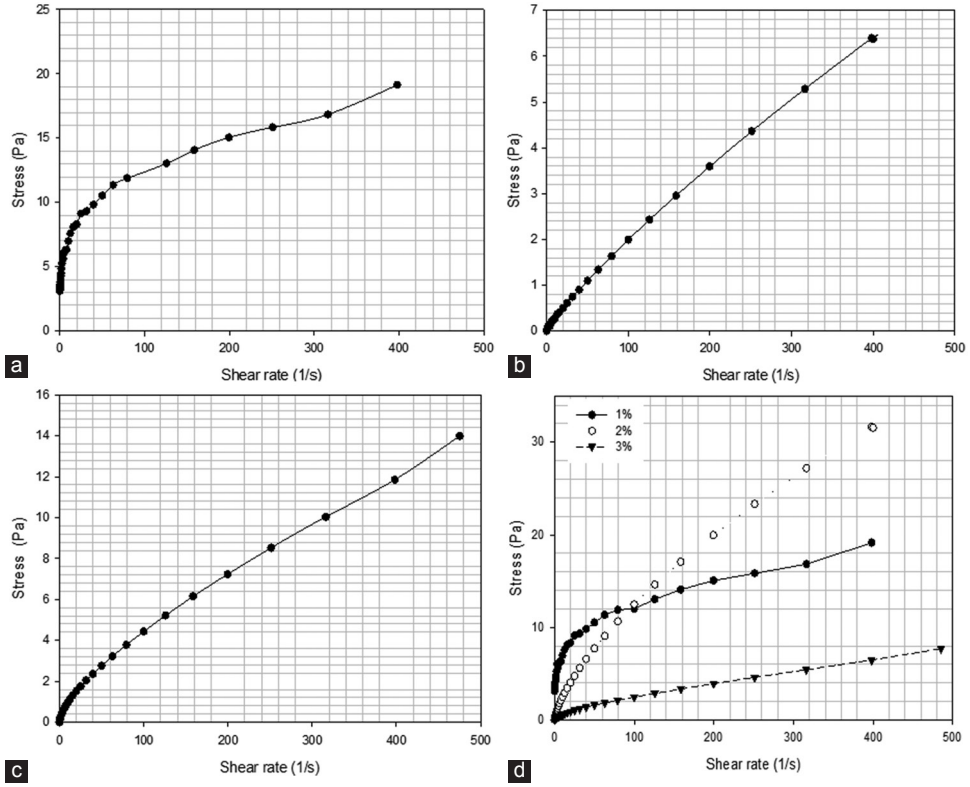

Figure 7. Stress versus shear rate for solutions containing different alginate methacrylate concentrations reacted for 24 h. (a) 1% w/v of alginate, (b) 2% w/v of alginate, (c) 3% w/v of alginate, (d) comparison of all compositions.

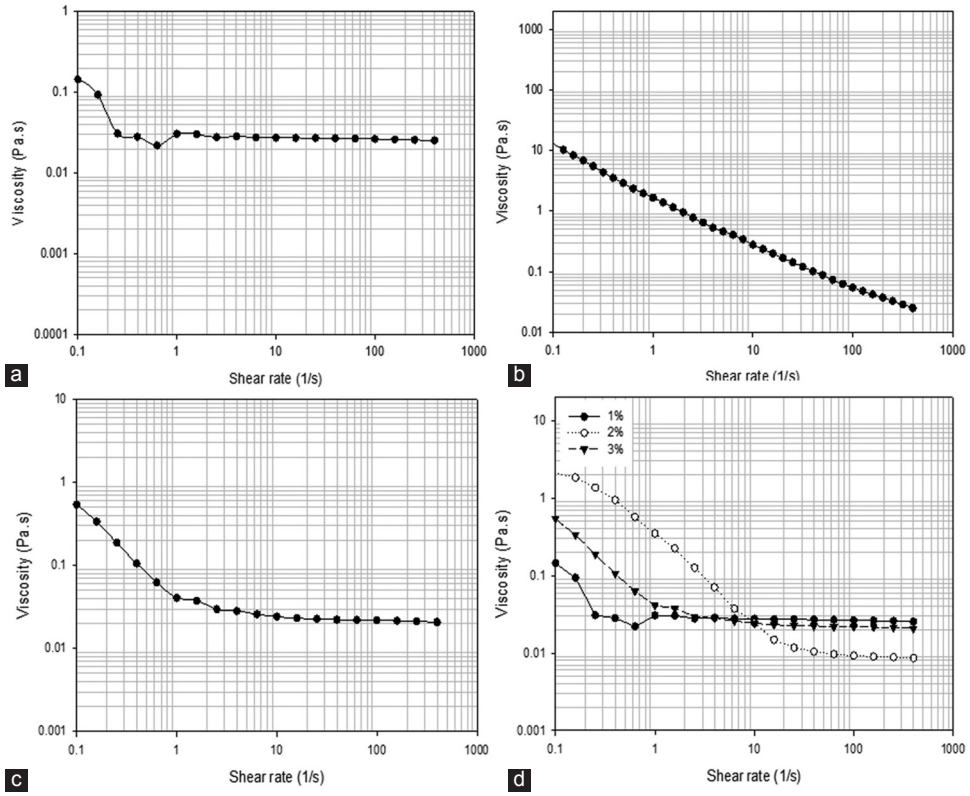

Figure 8. Viscosity versus shear rate for solutions containing different alginate methacrylate concentrations reacted for 8 h. (a) 1% w/v, (b) 2% w/v, (c) 3% w/v, (d) comparison of all compositions.

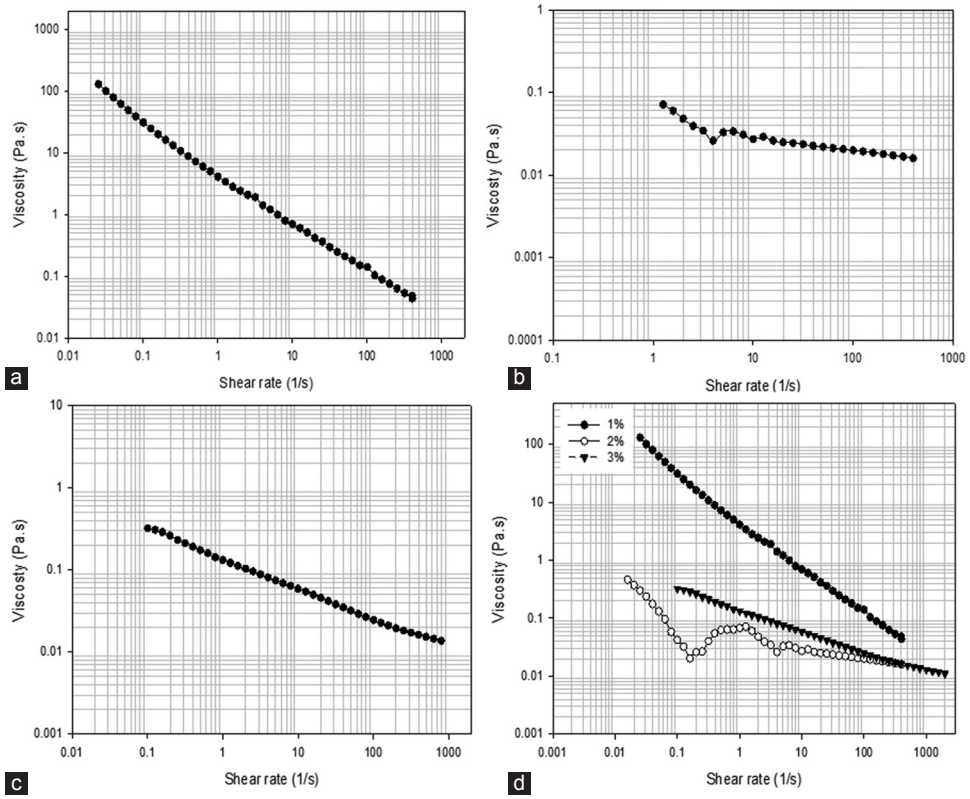

Figure 9. Viscosity versus shear rate for solutions containing different alginate methacrylate concentrations reacted for 24 h. (a) 1% w/v, (b) 2% w/v, (c) 3% w/v, (d) comparison of all compositions.

was selected as presents less variation of viscosity with the reaction time and a clear shear-thinning behavior being also less dependent with the reaction time compared to the other systems.

Figures 10 and 11 show the variation of storage modulus (G′), loss modulus (G″), complex modulus, and tan δ as a function of frequency and strain for systems containing 2% w/v alginate methacrylate concentrations

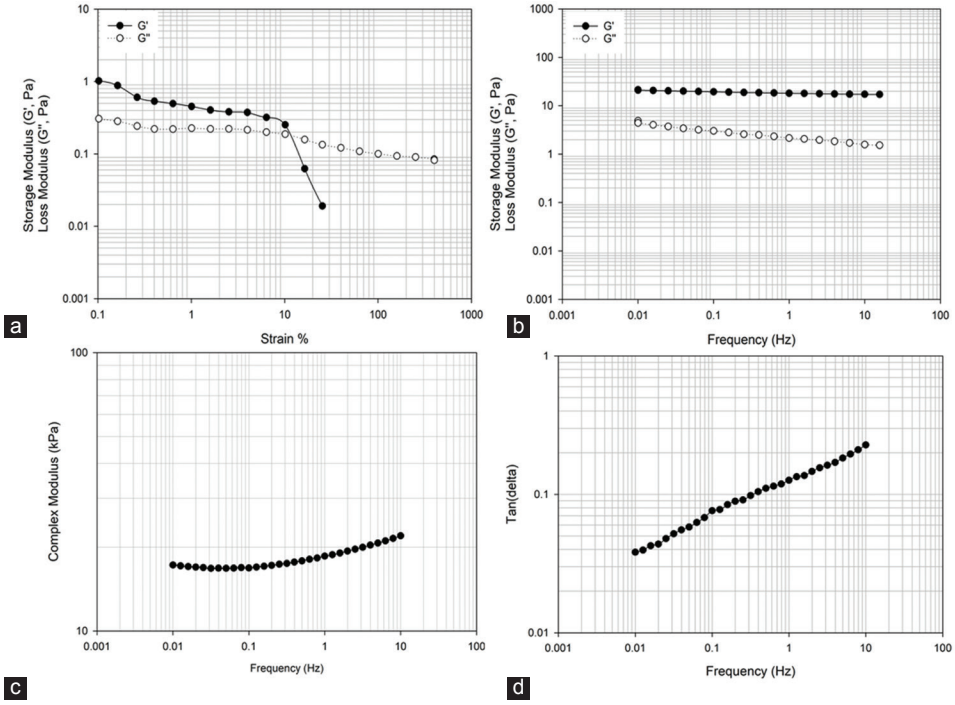

Figure 10. 2% wt. alginate solution reacted for 8 h. (a) storage and loss modulus versus strain (b) storage and loss modulus versus frequency, (c) complex modulus versus frequency, (d) tan δ versus frequency.

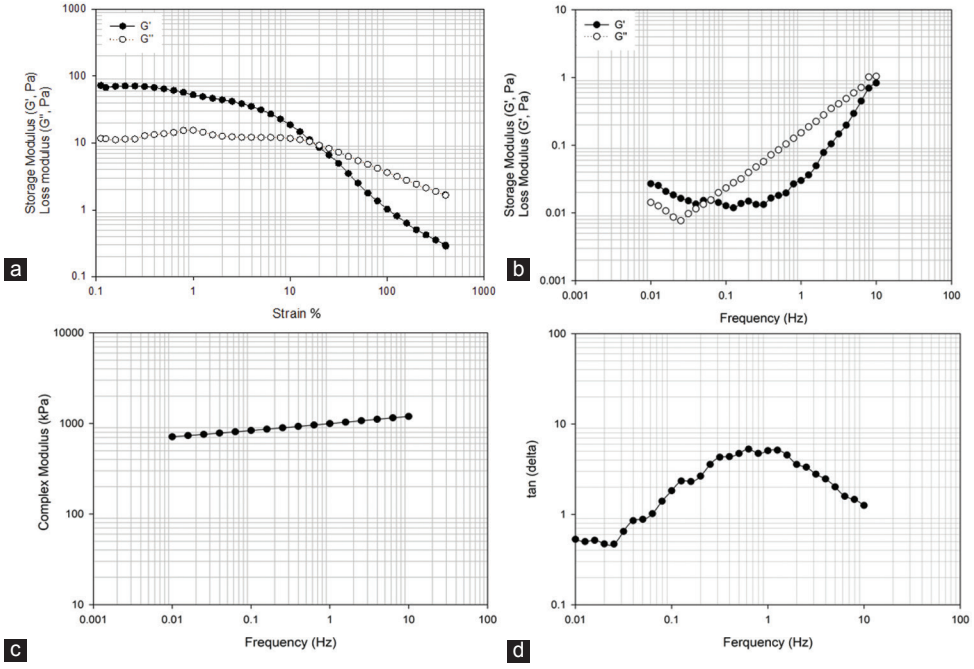

Figure 11. 2% wt. alginate solution reacted for 24 h. (a) storage and loss modulus versus strain, (b) storage and loss modulus versus frequency, (c) complex modulus versus frequency, (d) tan δ versus frequency.

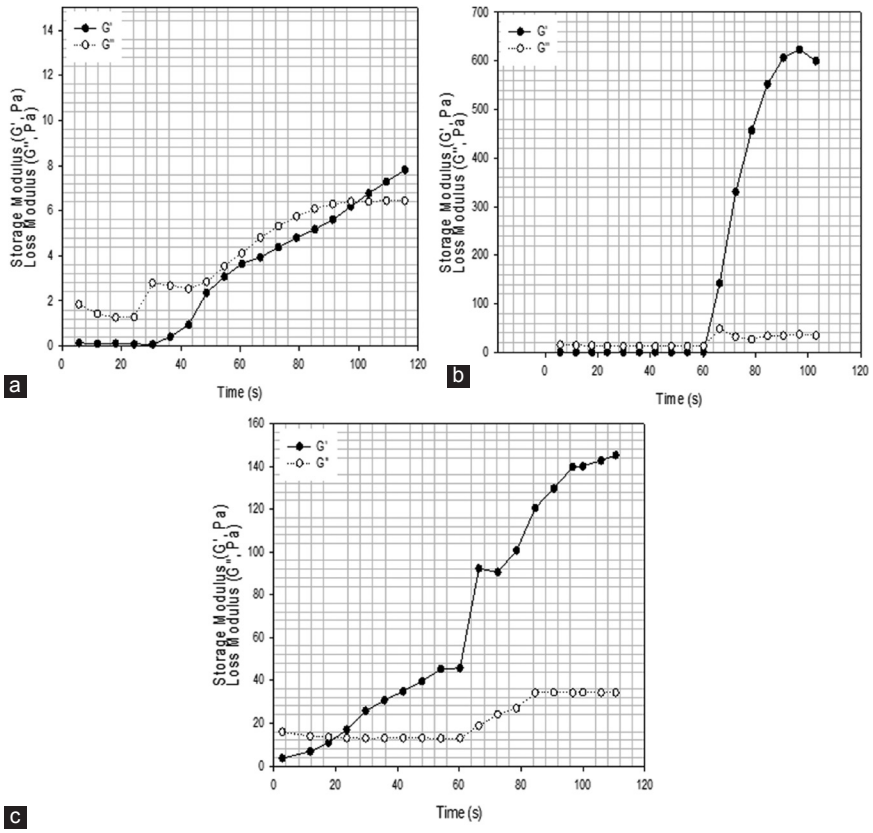

Figure 12. 2% wt. methacrylate alginate with different concentration of VA-086 photoinitiators functionalized for 8 h (a) 0.5% w/v of VA-086, (b) 1% w/v of VA-086, (c) 1.5% w/v of VA-086, d) 0.05%.

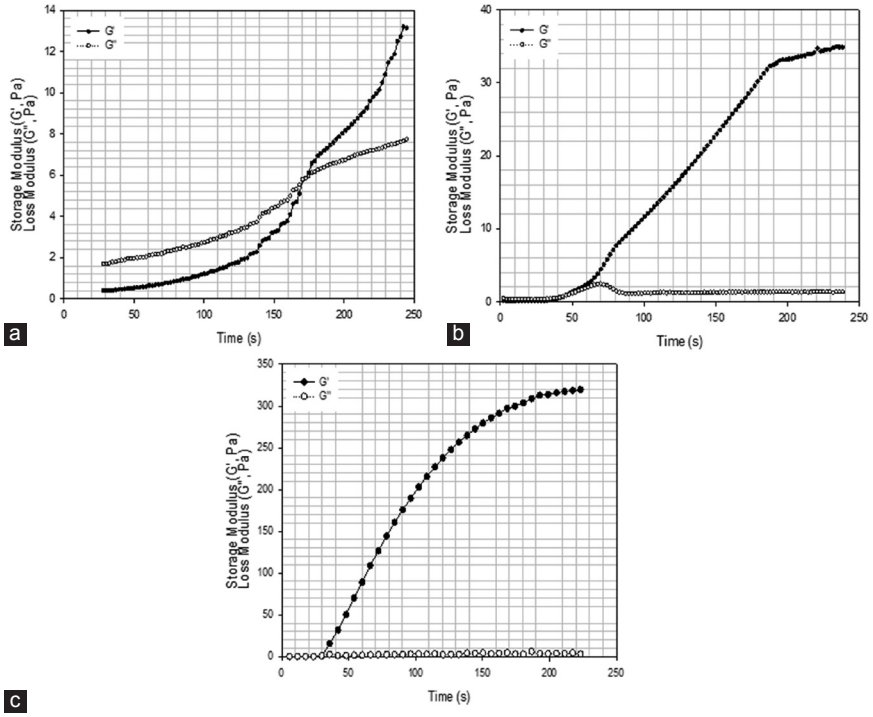

Figure 13. 2% wt. methacrylate alginate with different concentration of VA-086 photoinitiators functionalized for 8 h (a) 0.5% w/v of VA-086, (b) 1% w/v of VA-086, (c) 1.5% w/v of VA-086, (d) 0.05%.

and different reaction times. The results show that both the storage and loss modulus are higher in samples obtained after high functionalization times. In both cases, the complex modulus increases with frequency, while the variation of G′ and G″ with strain shows a shift point after which G″ becomes higher than G′. This shift occurs at high frequencies for alginate samples obtained with high functionalization times.

3.3 Rheological Changes during the Photopolymerization Process

Based on the characterization of the pre-polymerized samples, only systems containing 2% w/v of alginate were considered for photopolymerization studies. The curing kinetics was assessed by monitoring the variation of G′ and G″ at room temperature through a controlled frequency of (1Hz). Photorheology was used to characterize the curing process (photopolymerization) of functionalized alginate polymers obtained after 8 and 24 h of reaction time, mixed with 0.5-1.5% w/v, and of VA-086 photoinitiator solutions.

As observed from Figures 12 and 13 by increasing the curing time G′ increases becoming significantly higher than G″. It is also possible to observe that by increasing the photoinitiator concentration the gelation time, which corresponds to the time point where the G′ curve crosses the G″ curve, decreases. Notably observed that by increasing the amount of photoinitiators concentration G′ seems to tend to a plateau which corresponds to a verification stage of the curing process[35,36]. The possible explanation for this observation is that, for the layer thickness considered in this study (~100 μm), the photoinitiator concentration is approaching a critical value. By increasing the photoinitiator concentration above the critical values, the polymerization occurs very fast at the polymer surface, reducing the light penetration and, consequently, the overall polymerization reduces.

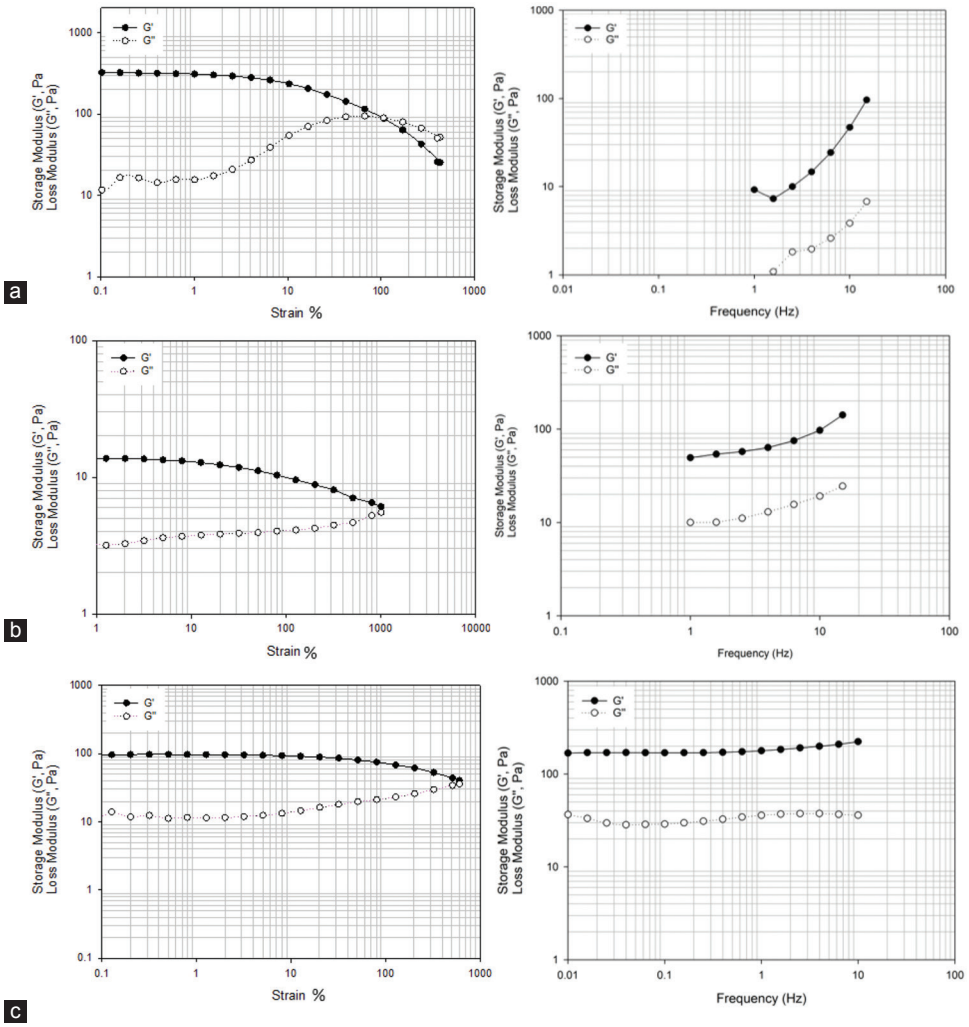

Figure 14. 2% wt. methacrylate alginate hydrogel with different concentration of VA-086 functionalized for 8 h. (a) 0.5 w/v % of VA-086, (b) 1 w/v % of VA-086, (c) 1.5 w/v % of VA-086.

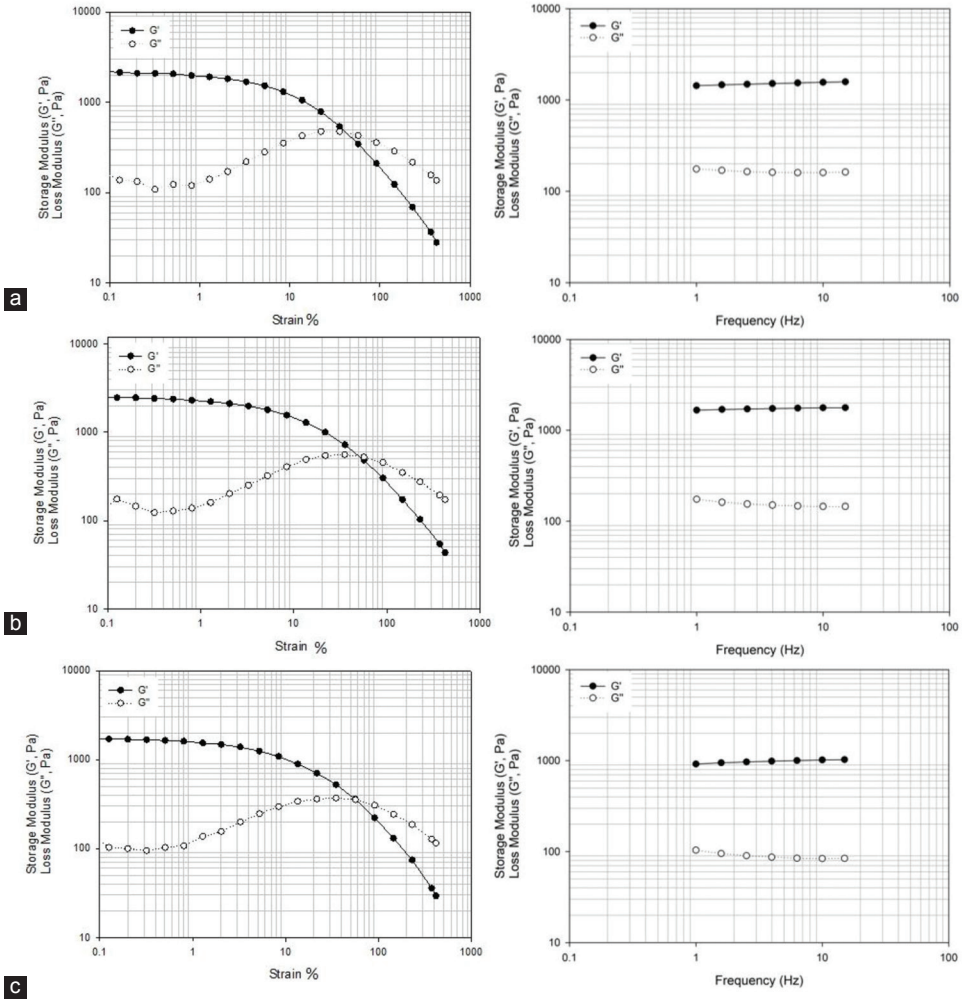

Figure 15. 2% wt. methacrylate alginate with different concentration of VA-086 functionalized for 24 h. (a) 0.5 w/v % of VA-086, (b) 1 w/v % of VA-086, (c) 1.5 w/v % of VA-086.

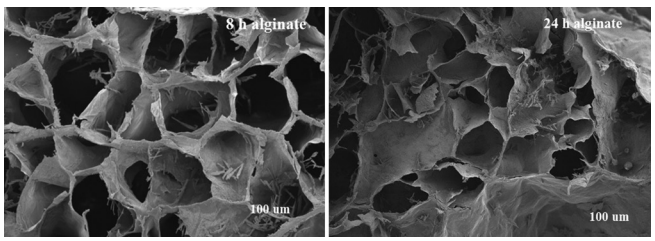

Figure 16. Scanning electron microscopy images of cross-linked methacrylate alginate hydrogel structures obtained from alginate-methacrylate at different reaction times: 8 and 24 h.

3.4 Viscoelastic Properties of Formed Hydrogels

Hydrogel disks (4 mm of height and 8 mm of diameter) were produced using an acrylic machined mold. Samples of 2 % w/v of alginate methacrylate obtained after both 8 and 24 h of reaction time containing different concentrations of photoinitiator (0.5, 1, and 1.5% w/v) were polymerized during 8 min under a light intensity of 8 mW/cm^2. Produced disks were then assessed and both G′ and G″ measured at room temperature through a controlled frequency of 1Hz as presented in Figures 14 and 15. In the case of alginate methacrylate samples obtained after 8 h of reaction time, its possible to observe that there is no significant change of both G′ and G″ (the storage modulus is always higher than the elastic modulus) with the increase in the photoinitiator concentration. In the case of alginate methacrylate samples obtained after 24 h of reaction time, results show that by increasing the photoinitiator concentration G′ and G″ increases. In this case, it is also possible to observe that the difference between G′ and G″ increases with the increase of photoinitiator concentration, which is associated with the high cross-linked density.

The viscoelastic nature of the cross-linked disks is also observed from the G′ and G″ versus strain graphs. In this case, it is possible to observe for all samples that, till a critical strain value, the storage modulus is

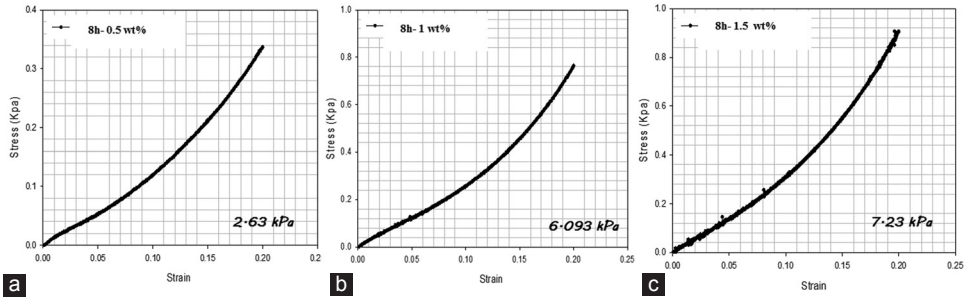

Figure 17. Compression tests for alginate methacrylate samples (8 h) with different photoinitiator concentrations (a) 0.5% w/v VA-086, (b) 1% w/v VA-086, (c) 1.5% w/v VA-086.

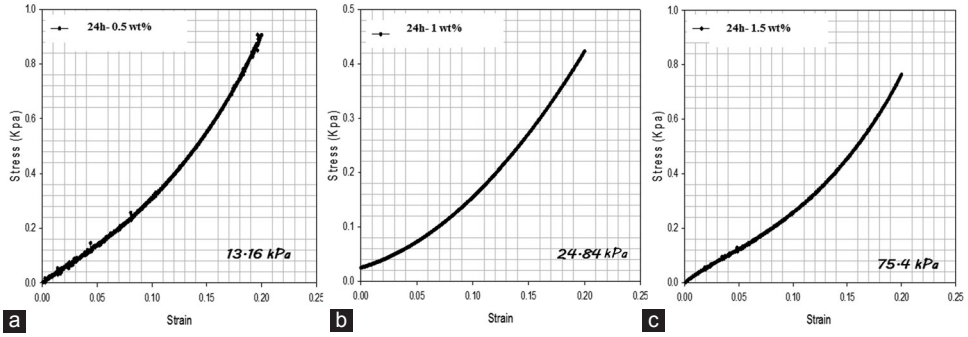

Figure 18. Compression tests for alginate methacrylate samples (24 h) with different photoinitiator concentrations (a) 0.5% w/v VA-086, (b) 1% w/v VA-086, (c) 1.5% w/v VA-086.

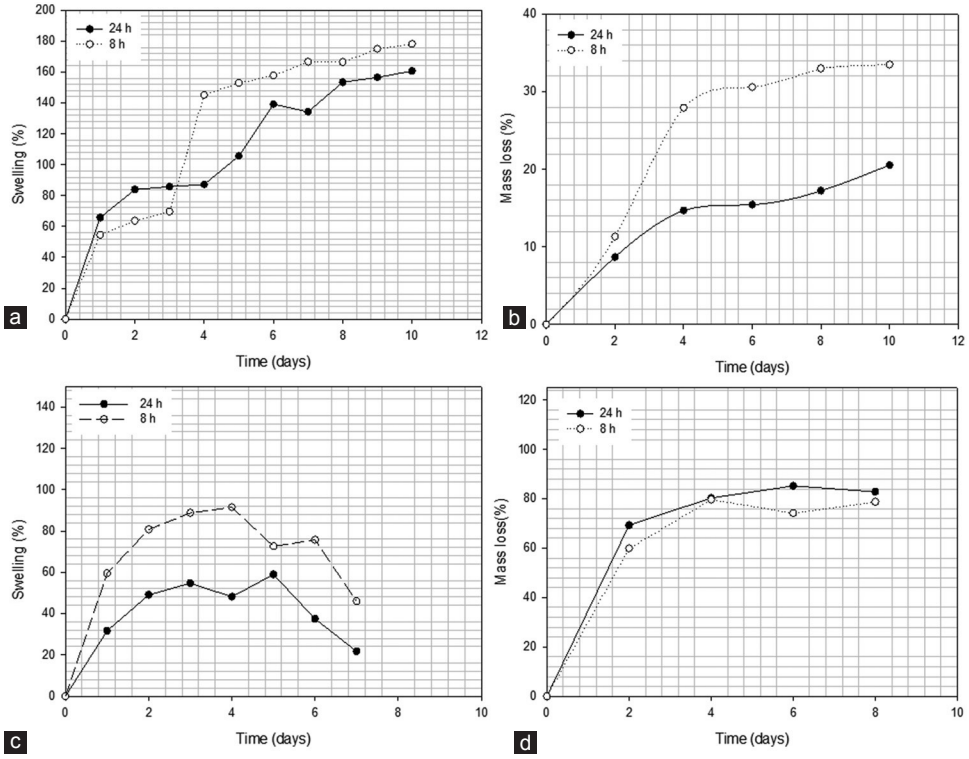

Figure 19. Swelling and degradation rate for 2% wt. functionalized alginate (24 and 8 h) reaction time in (a) distilled water (diH_2O), (b) degradation rate in diH_2O, (c) Dulbecco's Modified Eagle's Medium (DMEM), (d) degradation rate in DMEM.

higher than the loss modulus. After the strain critical value, the loss modulus becomes more significant due to the break of the cross-linked network. In the case of alginate methacrylate samples obtained after 24 h of reaction time, G′-24h modulus is always higher than G′-8h of alginate methacrylate samples obtained after 8 h of reaction time. This is due to the high-crosslinking density of the alginate methacrylate samples obtained after 24 h of reaction time.

3.5 Internal Morphology of Alginate Hydrogels

The internal structure of cross-linked alginate methacrylate is presented in Figure 16. SEM images were obtained for samples containing 2% w/v of alginate prepared during 8 and 24 h of reaction time and 1 w% of a photoinitiator. Results show that the reaction time influences the hydrogel morphology, with high reaction times being associated with structures presenting both small pore size and number of pores. In addition, results seem to indicate that long reaction times generate structures with more closed pores.

3.6 Mechanical Characterization

The mechanical performance of cross-linked alginate structures is presented in Figures 17 and 18. As observed, high compression moduli was obtained for cross-linked disks produced with high functionalization times (13.16 kPa for 24 h of reaction time and 2.63 kPa for 8 h of reaction time) and 0.5% w/v photoinitiator concentration. These results can be explained by the high crosslinking density that characterizes the structures obtained from alginate samples functionalized during long reaction times and the corresponding internal morphology characterized by small size and a low number of pores. It is also possible to observe that the mechanical properties increase by increasing the photoinitiator concentration. For samples containing 1.5% w/v of photoinitiator, compression moduli was obtained (75.4 kPa for 24 h of reaction time and 7.23 kPa for 8 h of reaction time).

3.7 Swelling and Degradation Kinetics

The swelling and degradation behavior of cross-linked alginate hydrogel disks are presented in Figure 19 (a,b,c and d). Results show that samples absorb both DMEM and diH_2O until reaching a state of equilibrium. This state is accomplished when the osmotic pressure from the swelling and the elasticity of the hydrogel network is equal. It is also possible to observe that cross-linked samples prepared with alginate methacrylate obtained after 24 h of functionalization present low swelling ratio, which shows that the degree of crosslinking controls the swelling properties of the hydrogel. In all samples, the equilibrium status was reached on day 3. Cross-linked alginate structures based on functionalized alginate prepared during 24 h of reaction time swelled up to 155%, while alginate structures based on functionalized alginate prepared during 8 h of reaction time swelled up to 190%. Moreover, it is also possible to observe that the level of functionalization of the pre-polymerized alginate not only determines the internal morphology of the cross-linked structures but also the degradation process as shown in Figure 19b and d.

4. Conclusion

This paper describes the synthesis and characterization of alginate systems for UV-based bioprinting applications. The alginate was successfully functionalized in the presence of methacrylate to introduce the necessary number of unsaturation allowing its crosslinking on photopolymerization. Two different functionalization reaction times were considered and photocurable systems containing different photoinitiator concentrations prepared. From the results, it is possible to conclude that high functionalization reaction times originates cross-linked structures with less porosity, smaller pores and a larger number of closed pores, less swelling, higher degradation properties, and higher mechanical stiffness. By increasing photoinitiator concentration, it was possible to observe an increase of mechanical properties and gelation time. Moreover, for high values of photoinitiator concentration, the reaction tends to reach verification.

Acknowledgment

Mr. H.H. Mishbak wishes to acknowledge the support of the Government of Iraq for supporting his PhD through a grant provided by the Higher Committee for Development Education Iraq. We would like to thank our colleagues from School of Materials, and the School of Mechanical, Aerospace, and Civil Engineering, The University of Manchester who provided insight and expertise with the mechanical compression test and rheological test that greatly assisted the research.

References

1. Pereira R, Bártolo PJF, 2015, 3D Bioprinting of Photocrosslinkable Hydrogel Constructs. *Appl Polym Sci,* 132(48):132A4. DOI 10.1002/app.42458.
2. Zhou D, Yoshihiro I, 2014, Visible Light-curable Polymers for Biomedical Applications. *Sci China Chem*, 57(4):510-21. DOI 10.1007/s11426-014-5069-z.
3. Pereira RF, Sousa A, Barrias CC, *et al*., 2018, A Single-component Hydrogel Bioink for Bioprinting of Bioengineered 3D Constructs for Dermal Tissue *Engineering*. *Mater Horiz,* 5(6):1100-11. DOI 10.1039/c8mh00525g.

4. Vyas C, Pereira R, Huang B, *et al*., 2017, *Engineering* the Vasculature with Additive Manufacturing. *Curr Opin Biomed Eng*, 2:1-13.
5. Wang W, Caetano G, Ambler W S, *et al*., 2016, Enhancing the Hydrophilicity and Cell Attachment of 3D Printed PCL/Graphene Scaffolds for Bone Tissue *Engineering*. *Materials (Basel, Switzerland)*, 9(12):992. DOI 10.3390/ma9120992.
6. Fand PR, Bártolo PJ, 2015, 3D Photo-fabrication for Tissue *Engineering* and Drug Delivery. *Engineering*, 1(1):90-112.
7. Dand NG, Bryant SJ, 2008, Cell Encapsulation in Biodegradable Hydrogels for Tissue *Engineering* Applications. *Tissue Eng Part B Rev,* 14(2):149-65. DOI 10.1089/ten.teb.2007.0332.
8. You F, Fand EB, Chen X, 2017, Application of Extrusion-based Hydrogel Bioprinting for Cartilage Tissue *Engineering*. *Int J Mol Sci,* 18(7):1597.
9. Highley CB, Rodell CB, Burdick JA, 2015, Direct 3D Printing of Shear-thinning Hydrogels into Self-healing Hydrogels. *Adv Mater,* 27(34):5075-9. DOI 10.1002/adma.201501234.
10. Pawar AA, Saada G, Cooperstein I, *et al*., 2016, High-performance 3D Printing of Hydrogels by Water-dispersible Photoinitiator Nanoparticles. *Appl Sci Eng,* 2(4):e1501381. DOI 10.1126/sciadv.1501381.
11. Banerjee A, Arha M, Choudhary S, *et al*., 2009, The Influence of Hydrogel Modulus on the Proliferation and Differentiation of Encapsulated Neural Stem Cells. *Biomaterials,* 30(27):4695-9. DOI 10.1016/j.biomaterials.2009.05.050.
12. Song SJ, Choi J, Park YD, *et al*., 2011, Sodium Alginate Hydrogel-based Bioprinting using a Novel Multinozzle Bioprinting System. *Artif Organs*, 35(11):1132-6. DOI 10.1111/j.1525-1594.2011.01377.x.
13. Pereira R, Tojeira A, Vaz DC, *et al*., 2011, Preparation and Characterization of Films Based on Alginate and *Aloe vera. Int J Polym Anal Charact*, 16(7):449-64.
14. Pereira R, Carvalho A, Vaz DC, *et al*., 2013, Development of Novel Alginate Based Hydrogel Films for Wound Healing Applications. *Int J Biol Macromol*, 52:221-30.
15. Pawar SN, Edgar KJ, 2012, Alginate Derivatization: A Review of Chemistry, Properties and Applications. *Biomaterials,* 33(11):3279-305. DOI 10.1016/j.biomaterials.2012.01.007.
16. Hermansson E, Schuster E, Lindgren L, *et al*., 2016, Impact of Solvent Quality on the Network Strength and Structure of Alginate Gels. *Carbohydr Polym,* 144:289-96. DOI 10.1016/j.carbpol.2016.02.069.
17. Hand D, Barikani M, 2012, Synthesis and Characterization of Calcium Alginate Nanoparticles, Sodium Homopolymannuronate Salt and its Calcium Nanoparticles. *Sci Iran,* 19(6):2023-8. DOI 10.1016/j.scient.2012.10.005.
18. Ouwerx C, Velings N, Mestdagh MM, *et al*., 1998, Physico-chemical Properties and Rheology of Alginate Gel Beads Formed with Various Divalent Cations. *Polym Gels Netw,* 6(5):393-408. DOI 10.1016/s0966-7822(98)00035-5.
19. Stagnaro P, Schizzi I, Utzeri R, *et al*., 2018, Alginate-polymethacrylate Hybrid Hydrogels for Potential Osteochondral Tissue Regeneration. *Carbohydr Polym,* 185:56-62. DOI 10.1016/j.carbpol.2018.01.012.
20. Yang X, Lu Z, Wu H, *et al*., 2018, Collagen-alginate as Bioink for Three-dimensional (3D) Cell Printing Based Cartilage Tissue *Engineering*. *Mater Sci Eng C,* 83:195-201. DOI 10.1016/j.msec.2017.09.002.
21. Müller M, Öztürk E, Arlov Ø, *et al*., 2017, Alginate Sulfate Nanocellulose Bioinks for Cartilage Bioprinting Applications. *Ann Biomed Eng,* 45(1):210-23. DOI 10.1007/s10439-016-1704-5.
22. Axpe E, Oyen ML, 2016, Applications of Alginate-based Bioinks in 3D Bioprinting. *Int J Mol Sci,* 17(12):e1976. DOI 10.3390/ijms17121976.
23. Szekalska M, Puciłowska A, Szymańska E, *et al*., 2016, Alginate: Current use and Future Perspectives in Pharmaceutical and Biomedical Applications. *Int J Polym Sci,* 2016:17. DOI 10.1155/2016/7697031.
24. Augst AD, Kong HJ, Mooney DJ, 2006, Alginate Hydrogels as Biomaterials. *Macromol Biosci,* 6(8):623-33.
25. Spadari CDC, Lopes LB, Ishida K, 2017, Potential use of Alginate-based Carriers as Antifungal Delivery System. *Front Microbiol*, 8:97. DOI 10.3389/fmicb.2017.00097.
26. Mishbak CVH, Cooper G, Bartolo P, 2019, Development and Characterisation of a Photocurable Gelatin/Alginate Bioink for 3D Bioprinting, Prof Dimiter Dimitrov D HH. In: von Leipzig K, editor. *Department of Industrial Engineering Stellenbosch University. International Conference on Competitive Manufacturing (COMA 19)*. DOI 10.18063/ijb.v5i2.189.
27. Jeon O, Bouhadir KH, Mansour JM, *et al*., 2009, Photocrosslinked Alginate Hydrogels with Tunable Biodegradation Rates and Mechanical Properties. *Biomaterials,* 30(14):2724-34. DOI 10.1016/j.biomaterials.2009.01.034.
28. Benton JA, DeForest CA, Vivekanandan V, *et al*., 2009, Photocrosslinking of Gelatin Macromers to Synthesize Porous Hydrogels that Promote Valvular Interstitial Cell Function. *Tissue Eng Part A,* 15(11):3221-30. DOI 10.1089/ten.tea.2008.0545.
29. Sudhakar CK, Upadhyay N, Jain A, *et al*., 2015, Hydrogels Promising Candidates for Tissue *Engineering*. In: Thomas S, Grohens Y, Ninan N, editors. *Nanotechnology Applications*

for Tissue Engineering. Ch. 5. William Andrew Publishing, Oxford, p77-94. DOI 10.1016/b978-0-323-32889-0.00005-4.

30. Bonino CA, Samorezov JE, Jeon O, *et al*., 2011, Real-time in Siturheology of Alginate Hydrogel Photocrosslinking. *Soft Matter,* 7(24):11510-7. DOI 10.1039/c1sm06109g.
31. Smeriglio P, Lai JH, Yang F, *et al*., 2015, 3D Hydrogel Scaffolds for Articular Chondrocyte Culture and Cartilage Generation. *J Vis Exp*, 104:53085. DOI 10.3791/53085.
32. Çiğdem KM, Doğan Ö, Faika DS, 2013, Comparison of Chemical Fractionation Method and 1H-NMR Spectroscopy in Measuring the Monomer Block Distribution of Algal Alginates. *J Polym Eng,* 33(3):239-46. DOI 10.1515/polyeng-2012-0066.
33. Smeds KA, Pfister-Serres A, Miki D, *et al*., 2001, Photocrosslinkable Polysaccharides for in situ Hydrogel Formation. *J Biomed Mater Res,* 55(2):254-5. DOI 10.1002/1097-4636(200105)55:2<254::aid-jbm1012>3.0.co;2-5.
34. Lam C, Jefferis SA, 2014, Interpretation of Viscometer Test Results for Polymer Support Fluids. *Tunneling Undergr Constr,* 2014:439-49. DOI 10.1061/9780784413449.043.
35. Bartolo P, Lenz EJC, 2006, Computer Simulation of Stereolithographic Curing Reactions: Phenomenological Versus Mechanistic Approaches. *CIRP Ann,* 55(1):221-5. DOI 10.1016/s0007-8506(07)60403-x.
36. Matias JM, Bartolo PJ, Pontes AV, 2009, Modeling and Simulation of Photofabrication Processes using Unsaturated Polyester Resins. *Appl Polym Sci,* 114(6):3673-85. DOI 10.1002/app.30405.